Unclassified
SECURITY CLASSIFICATION OF THIS PAGE

(2)

REPORT DOCUMENTATION PAGE

AD-A210 245

ILE

1b RESTRICTIVE MARKINGS: None

3. DISTRIBUTION / AVAILABILITY OF REPORT: Approved for public release and sale. Distribution unlimited.

4. PERFORMING ORGANIZATION REPORT NUMBER(S): ONR Technical Report No. 12

5. MONITORING ORGANIZATION REPORT NUMBER(S)

6a. NAME OF PERFORMING ORGANIZATION: University of Utah

6b. OFFICE SYMBOL (*If applicable*)

7a. NAME OF MONITORING ORGANIZATION

6c. ADDRESS (*City, State, and ZIP Code*): Department of Chemistry, Henry Eyring Building, Salt Lake City, UT 84112

7b. ADDRESS (*City, State, and ZIP Code*)

8a. NAME OF FUNDING / SPONSORING ORGANIZATION: Office of Naval Research

8b. OFFICE SYMBOL (*If applicable*)

9. PROCUREMENT INSTRUMENT IDENTIFICATION NUMBER: N00014-89-J-1412

8c. ADDRESS (*City, State, and ZIP Code*): Chemistry Program, Code 1113, 800 N. Quincy Street, Arlington, VA 22217

10. SOURCE OF FUNDING NUMBERS

PROGRAM ELEMENT NO.	PROJECT NO.	TASK NO.	WORK UNIT ACCESSION NO

11. TITLE (*Include Security Classification*): **Multiple Internal Reflection Fourier Transform Infrared Spectroscopy Studies of Thiocyanate Adsorption on Silver and Gold**

12. PERSONAL AUTHOR(S): D. B. Parry, J. M. Harris and K Ashley

13a. TYPE OF REPORT	13b. TIME COVERED	14. DATE OF REPORT (*Year, Month, Day*)	15. PAGE COUNT
Technical	FROM 7/88 TO 7/89	July 1, 1989	38

16. SUPPLEMENTARY NOTATION

17 COSATI CODES		
FIELD	GROUP	SUB-GROUP

18. SUBJECT TERMS (*Continue on reverse if necessary and identify by block number*): Infrared spectroscopy of liquid/solid interfaces, ionic adsorption in the double-layer region.

19. ABSTRACT (*Continue on reverse if necessary and identify by block number*)

Attached.

20. DISTRIBUTION / AVAILABILITY OF ABSTRACT: ☒ UNCLASSIFIED/UNLIMITED ☐ SAME AS RPT ☐ DTIC USERS

21. ABSTRACT SECURITY CLASSIFICATION: Unclassified

22a. NAME OF RESPONSIBLE INDIVIDUAL: Dr. Robert J. Nowak

22b. TELEPHONE (*Include Area Code*): (202) 696-4410

22c. OFFICE SYMBOL

DD FORM 1473, 84 MAR — 83 APR edition may be used until exhausted. All other editions are obsolete.

SECURITY CLASSIFICATION OF THIS PAGE
Unclassified

OFFICE OF NAVAL RESEARCH

Grant No: N00014-89-J-1412

R&T Code 413a005---03

Technical Report No. 12

Multiple Internal Reflection Fourier Transform Infrared Spectroscopy Studies of Thiocyanate Adsorption on Silver and Gold

Prepared for publication in Langmuir

by

D. B. Parry, J. M. Harris, and K. Ashley

Department of Chemistry
University of Utah
Salt Lake City, UT 84112

July 1, 1989

MULTIPLE INTERNAL REFLECTION FOURIER TRANSFORM INFRARED SPECTROSCOPY STUDIES OF THIOCYANATE ADSORPTION ON SILVER AND GOLD

Diane B. Parry and Joel M. Harris*
Department of Chemistry
University of Utah
Salt Lake City, UT 84112

and

Kevin Ashley*
Department of Chemistry
San Jose State University
San Jose, CA 95192

ABSTRACT

Conducting silver and gold coatings on silicon Attenuated Total Reflectance (ATR) plates have been employed as transparent electrodes to monitor *in situ* surface electrochemistry. The multiple internal reflection Fourier transform infrared spectroscopy (MIRFTIRS) technique, used previously to study redox reactions on platinum and iron films, is applied in this work to the study of adsorption processes in the double-layer region, in particular, the adsorption of thiocyanate on silver and gold. The MIRFTIRS spectra were found to be essentially free of solution band interference and are compared to surface IR spectra of the same system obtained by other methods. Spectra of thiocyanate adsorbed on gold and silver surfaces have been recorded as a function of applied potential and thiocyanate concentration. Evidence of thiocyanate species absorbed to gold via both nitrogen and sulfur atoms has been obtained, while only S-bound thiocyanate was clearly observed on silver.

INTRODUCTION

The spectroelectrochemical technique, Multiple Internal Reflection Fourier Transform Infrared Spectroscopy (MIRFTIRS), has previously been employed in redox studies involving iron and platinum films (1-3). The sensitivity and surface selectivity of MIRFTIRS, however, suggest that it has much broader applications, both in terms of the chemical systems which can be studied and the combinations of metal films and ATR substrates available. The method is applied here to study adsorption of thiocyanate on silver and gold films within limits of applied potential where no Faradaic processes occur.

One of the major advantages of internal reflection methods is the ability to control the depth of penetration of the evanescent wave past the surface which makes it possible to avoid intense interference from solution bands. The combination of the multiple reflection technique with FTIR improves signal/noise and the speed at which data can be collected. In addition to the surface specificity, signal/noise improvement, and speed advantages of MIRFTIRS, electrodes of a variety of different metals are easily prepared by vapor-depositing or sputter-coating thin films on cleaned silicon (or other suitable material) ATR plates.

Another major advantage of the MIRFTIRS spectroelectrochemical technique is the geometry of the electrochemical cell. The cell configuration favors a uniform potential distribution across the face of the working electrode (the thin metal film). An uneven potential distribution may exist across the electrode surface in an external reflection geometry due to the finite IR drop through the thin solution layer trapped between the electrode surface and the cell window.

The use of ATR methods with thin metal film electrodes is a well established approach to spectroelectrochemical studies. The electrochemical method most

often explored and most closely related to MIRFTIRS, which demonstrates surface-specificity in the infrared, is the single-reflectance Kretschmann configuration ATR method. The Kretschmann configuration has been used to probe thiocyanate adsorption on silver and gold films (4,5). The advantages of MIRFTIRS over the Kretschmann configuration are that the increased number of internal reflections improves signal/noise. Multiple reflections also insure that data are generated from a representative sample of the electrode surface, which prevents misleading spectra from chemistry occurring at one specific site on an electrode surface (6).

Although optically transparent metal films on multiple internal reflection ATR plates have seldom been used in spectroelectrochemical experiments, many multiple-reflection ATR electrochemical studies have been performed without the use of metal films. These investigations have been limited to semiconducting electrodes. Several types of the commercially available ATR plate materials have been studied. For example, ZnO crystals (7), tin oxide (an n-type semiconductor) coatings on glass (8), silicon (9-12), and germanium (13) were all used in ATR electrochemical experiments after the pioneering work on germanium by Mark and Pons in 1966 (14). A recent and more detailed review of semiconductor-electrolyte interface studies is available (15).

Since the benefits of multiple-internal reflection are well known in semiconductor electrochemistry, the development of MIRFTIRS with fully conducting, optically transparent metal films seems a reasonable solution to some of the specificity and sensitivity problems encountered in surface adsorption spectroelectrochemistry. The choice of thiocyanate as an example system for study was based on the window of spectral transparency of silicon in the infrared, and on the availability of data from previous studies performed on

thiocyanate for comparison with data collected in this work. The silicon ATR substrate is optically transparent to infrared radiation at frequencies only above ~1600 cm^{-1}; low wavenumber information is unavailable using a silicon ATR plate. Detection of thiocyanate C≡N stretching mode (occurring between 2000-2200 cm^{-1}) is compatible with the infrared window of silicon. The hardness of silicon, however, makes it an ideal substrate for control of thin metal film deposition. Softer ATR substrate materials were found to require vapor-deposition of thicker metal layers in order to yield films which are conductive. Thinner metal films have the advantage of allowing greater infrared intensity to interrogate the metal/solution interface than thicker metal layers.

The second reason for studying thiocyanate adsorption is the large body of information on the adsorption of this ion on a variety of metals as discussed in a recent review (16), and in publications dealing specifically with thiocyanate adsorption on silver and gold (4,5,17-19). While a great deal of data exists for thiocyanate adsorption, discrepancies exist in the interpretation of the results from different methods used to study the same system. The spectroelectrochemical methods which have been used to probe this system include subtractively normalized interfacial Fourier transform infrared spectroscopy (SNIFTIRS) (18a), surface-enhanced Raman spectroscopy (SERS) (17,18a), Fourier transform infrared reflection absorption spectroscopy (FT-IRRAS) (19), and the Kretchmann ATR prism configuration method (4). Choosing a system studied by other spectroelectrochemical methods prior to this work allows direct comparisons between MIRFTIRS and other spectroelectrochemical methods.

EXPERIMENTAL

Materials. Sodium thiocyanate was used as received from EM Science. Sodium perchlorate, hydrated, was used as received from the G. Frederick Smith Chemical Company. Chemicals used in cleaning the silicon substrate include 30% hydrogen peroxide from Malinckrodt, and hydrofluoric acid, ammonium hydroxide, nitric acid, and hydrochloric acid, (reagent grade) from J.T. Baker. These materials were used as received. Water for these experiments was from a NANOpure II water purification system from Barnstead.

The polycrystalline silicon substrates, part number EE3131, were obtained from Harrick Scientific Corporation. Each substrate was a 50x20x3 mm, 45°, single pass parallelepiped plate.

Substrate modification. Prior to vapor-depositing thin silver or gold films on the silicon substrate, previously deposited metal films were removed by several minutes of soaking in an Aqua Regia bath. The teflon components of the spectroelectrochemical cell were also rinsed with Aqua Regia. The silicon substrate was cleaned by procedures that have been described elsewhere (20).

Although no oxide layer was intentionally grown on the silicon ATR plate, a silicon oxide layer (~10A as determined by ellipsometry) has been shown (21) to grow under ambient conditions on clean silicon substrates. To remove this oxide layer, the crystal was placed in a solution of 1:50 HF:H_2O, so that any oxide layer present was removed. This procedure was carried out immediately before placing the ATR plate in the vacuum system.

An Edwards model E306A vacuum coating unit was used to vapor deposit thin films of silver (99.99+ % wire) and gold (99.99+ % wire) onto the cleaned silicon ATR plates. Films were deposited immediately before each experiment, and each film was used only once. The thickness of the silver and gold layers deposited

were measured by an Edwards model FTM5 thickness monitor. Both metals were deposited at a rate of ~4 nm/sec under a vacuum of 5 x 10^{-5} torr. For silver film experiments, the thickness of the silver layer was 205 $\pm$ 2 nm, and for gold the thickness deposited was 225 $\pm$ 3 nm.

ATR-FTIR. The FTIR system used was a Bio-Rad, Digilab division, FTS-40 equipped with a 3240 SPC data system. Spectra were obtained at a resolution of 4 cm^{-1}. A variable angle ATR attachment designed to fit the FTIR was a model 301 from Spectra-Tech. The spectroelectrochemical cell used is illustrated in Figure 1. In addition to the metal-coated ATR substrate serving as the working electrode, the cell contained a platinum counter electrode, and a saturated calomel reference electrode (SCE).

MIRFTIR Measurements. The ATR spectroelectrochemical cell containing the metal-film coated crystal was placed and aligned in the dry air purged sample compartment of the spectrophotometer. The cell was filled with a freshly prepared NaSCN/$NaClO_4 \cdot H_2O$ solution (the perchlorate concentration was 0.15 M in all experiments, and the NaSCN concentration was varied between 1, 10 and 25 mM, as labeled on the spectra). Once introduced into the cell, the electrolyte solutions were degassed with pure nitrogen before each experiment. The electrochemical potential was controlled by an IBM Instruments model EC225[1a] Voltammetric Analyzer. A silver wire was clamped to an edge of the ATR plate in such a way that the wire contacted the metal film surface. The completeness of this connection was tested with a continuity tester. No epoxy, glue, or solder was necessary. The background spectrum was collected at zero potential versus the SCE reference. All potentials reported here are versus the SCE reference. For each potential, 256 interferograms were collected and averaged.

RESULTS AND DISCUSSION

The MIRFTIRS Technique

The MIRFTIRS technique appears to provide several important attributes for spectroelectrochemical studies: 1) its surface selectivity limits the solution band interference, 2) the multiple reflections effectively increase the signal-to-noise ratio, and 3) an even potential distribution is achieved across the face of the electrode. This section will provide a discussion of the data in terms of these benefits, while comparing MIRFTIRS with techniques previously employed.

Figures 2 through 7 show the infrared difference spectra of SCN^- adsorbed from electrolyte solutions of varying concentrations (as labeled on the figures) on both silver and gold electrodes; the reference spectrum used to generate the difference spectra was collected under identical conditions at zero volts versus SCE. On both metals, the signal to noise is very good for 25 and 10 mM NaSCN solutions and peaks can be seen on the spectra from films of both metals at the 1 mM concentration level. The signal/noise ratio of the MIRFTIRS system appears to be improved over the data obtained by the Kretschmann prism configuration for the same NaSCN solution concentration on gold (5) and on silver (4). Unfortunately, these references (4,5) do not state the number of spectra collected using the Kretschmann method. The Kretschmann configuration generates data with superior signal/noise over the Fourier transform IRRAS technique in thiocyanate on silver electrodes (4).

Solution phase species can interfere with the collection of spectroelectrochemical data of surface adsorbed species. Thiocyanate ion in aqueous solution has a band at about 2065 cm^{-1} (18, 19, 22) which is generally not seen using MIRFTIRS. To test the position of the solution band in the ATR arrangement, a cleaned silicon substrate which had not been coated with a thin

metal film was placed in the electrochemical cell. The cell was filled with 10mM NaSCN in 0.15 M $NaClO_4$. A background collected from the empty cell was subtracted from a spectrum of the NaSCN-containing cell. The solution peak was found to appear at 2065 cm^{-1}, with a weak intensity of 4 X 10^{-4} absorbance units. For the geometry of these MIRFTIRS experiments, a calculation of the depth of penetration, d_p, the distance into the solution at which the evanescent wave intensity drops by a factor of e^{-2} (23), indicates that between 2000 and 2500 cm^{-1}, d_p is in the range 0.31-0.38 μm. The interface was modeled as a silicon/water boundary in these calculations, since the thickness of the silver or gold films are only about 4% of the wavelength of light, and $NaClO_4$ and NaSCN are present at low concentrations. The refractive indices of silicon (24) and water (25) were found in the literature. The very small depth of penetration of the evanescent wave into the solution explains the weak intensity of the solution band detected in this experiment.

Some evidence of solution interference may be seen in the -0.5 volt potential spectrum of 25 mM thiocyanate on gold (see Figure 8a) and possibly in spectra collected at the same potential on silver (Figure 8b), but the presence of the solution band does not interfere with the interpretation of the adsorbed species. The peak assigned as a solution band in Figure 8a (SCN^- on Au) occurs at ~2070 cm^{-1}, and in Figure 8b (SCN^- on Ag) the peak nearest the solution band frequency occurs at ~2087 cm^{-1}. The 2087 cm^{-1} peak in the silver experiments is to high in frequency to be assigned to the solution species, and will be discussed further below. The presence of adsorbed species throughout the double layer region studied here is indicated by differential capacitance data for both Ag (26) and Au (18), which show that thiocyanate is adsorbed on the electrode surface at all potentials within the double layer region. Since most of the

spectra presented (Figures 2-7) here show little or no solution interference, and since capacitance data confirm that adsorbed species are present, the peaks occurring in Figures 2-7 above 2070 cm^{-1} are assigned to adsorbed species. The designation of peaks existing at wavenumbers higher than 2070 cm^{-1} as adsorbed species is reinforced by the fact that adsorbed species change frequencies with changes in potential, while solution peak frequencies do not respond to changes in potential. All of the peaks assigned as surface species here show a definite shift in energy as the electrode potential is changed from positive to negative values.

At first glance, some discrepancies appear between the difference spectra presented here and the SNIFTIRS data from the same systems (18, 19). The SNIFTIRS data shows the presence of a strong solution band, with a maximum at 2064 cm^{-1} on gold (18) and at approximately the same frequency on silver (19); note that this frequency corresponds to the solution-phase thiocyanate species. In the SNIFTIRS experiment on silver (19), the distance through the solution that the IR beam traveled was given as 100 μm (twice the distance, 50μm, between the optical window of the cell and the electrode). However, this distance does not reflect the SNIFTIRS cell geometry precisely, since the cell window and the electrode surface are not necessarily parallel, allowing for significant differences in IR path length at various points on the electrode surface. As described above, our depth of penetration into the solution in the spectral region of interest is between 0.31 and 0.38 μm, so it is reasonable that the SNIFTIRS technique should suffer more from solution band interference than the MIRFTIRS method. We observe a ten-fold attenuation of the solution band peak with the MIRFTIRS data over that of the SNIFTIRS data given in the literature (19). This suggests that the actual pathlength of infrared light through the

SNIFTIRS cell, as it was assembled in the experiments documented (19), was less than 10 μm.

A shoulder on the apparent solution band in SNIFTIRS experiments on gold occurs at 2106 cm^{-1} (18), the same position as a peak observed in the present work (see Figure 2). Figures 2, 3, and 4 show peaks in the 2125-2133 cm^{-1} range (although none occurred above 2133 cm^{-1}), and in the 2112-2122 cm^{-1} range, as reported previously in the SNIFTIRS results (18, 19). The absence of the solution band near 2065 cm^{-1} in the data presented here make band assignments more straightforward than in the SNIFTIRS data (18, 19). Spectra from thiocyanate adsorbed on silver reported for the SNIFTIRS technique (19) are noisier than the MIRFTIRS data and more difficult to compare. The principal difficulty in comparing SNIFTIRS and MIRFTIRS data, however, is that the silver SNIFTIRS data have significant interference from the solution band, which obscures the region of interest.

Thiocyanate Adsorption on Silver

While many similarities exist in the adsorption of thiocyanate to silver and gold, it is convenient to examine each system separately. At the silver electrode with a 25 mM NaSCN concentration (Figure 2), as the potential was tuned from +0.2 volts to -0.6 volts, the strongest band, which gains intensity at positive potentials and looses intensity at negative potentials compared to the zero volt reference spectrum, shifts from 2124-2114 cm^{-1} ($d\nu/dE$ = 12 $cm^{-1} \cdot V^{-1}$). This peak is assigned as the S-bound thiocyanate species, since S-bound thiocyanate has been determined to be the predominant surface species at more positive potentials (4,5,18), and since the peak position shifts with potential. Assignments of vibrations as surface species are made only for those peaks which shift with potential, since frequencies of solution species do not shift with

potential (16). The peak-to-peak value of 12 $cm^{-1} \cdot V^{-1}$ for $d\nu/dE$ is similar to values reported elsewhere for the S-bound thiocyanate (22, 18a). Frequency and intensity data for 25 mM, 10 mM and 1 mM NaSCN solutions are listed in Table I.

The only other spectral feature, which is seen as a weak positive peak in the 25 mM and 10 mM concentration data, is the small peak which appears to shift from 2102-2087 cm^{-1} between -0.1 volts and -0.6 volts ($d\nu/dE$ = 15 $cm^{-1} \cdot V^{-1}$) (see Figure 3). This feature is not observed at positive potentials. The ~2087 cm^{-1} peak is a weak feature compared to the S-bound thiocyanate peak, and it is not observed in the 1mM data. This peak is most prominent in the 10mM data (as the results are presented here), although it is more apparent in the 25 mM results when the spectra are expanded, as shown in Figure 8b.

The 2087 cm^{-1} peak might be assigned as a solution band, since a very broad feature is seen at 2080 cm^{-1} in the spectra collected at more positive potentials. At positive potentials above +0.2 volts, the silver layer begins form AgSCN or a precursor and leave the surface (17). Figure 9 shows spectra of thiocyanate on the silver electrode at the potentials +0.3 and +0.4 volts. The large positive peaks at 2144 cm^{-1} are assigned to the presence of AgSCN complexes on the electrode surface. Once these vibrational bands are observed, the electrode no longer functions electrochemically, and removing the substrate from the cell reveals a gray, easily removable material on the silicon surface. Assignment of the AgSCN peak frequency is based on data reported elsewhere (17), where the AgSCN band was reported to be 2140 cm^{-1}. These literature data agree well with the 2144 cm^{-1} peak reported here (see Figure 9). The relatively weak, broad feature centered at 2080 cm^{-1} could be due to solution species produced when silver has left the electrode. It could also be due to changes in the background spectrum occurring from loss of the silver layer.

The assignment of the ~2087 cm^{-1} peak as a solution band is less supportable, however, if all of the data collected here are considered. In the discussion above, it was reported that the frequency of this band changed with potential. Since only surface species show changes in frequency with potential, and since it has been shown on gold that N-bound species exist at more negative potentials (18), the ~2087 cm^{-1} band may be due to N-bound thiocyanate on the surface. Additional data to support the N-bound thiocyanate claim are: 1) a solution spectrum was collected for this system with a peak appearing at 2065 cm^{-1}, a significantly lower frequency than the ~2087 cm^{-1} peak under discussion, and 2) Ashley et al. (22) have observed that N-bound thiocyanate shifts further with potential than the S-bound species and in the same frequency direction reported here. The greater frequency shift of the N-bound over the S-bound peaks is predicted by the Gouy-Chapman-Stern model of the electrochemical interface (27). The Gouy-Chapman-Stern model assumes that the magnitude of the potential drop across the double-layer region is greatest near the electrode surface. In the case of thiocyanate, the electric field which the C-N oscillator experiences is greatest in the N-bound configuration, which induces the peak frequency to change more with potential (in this case, the N-bound shifts 15 cm^{-1} V^{-1} and the S-bound shifts 12 cm^{-1} V^{-1}).

While the assignment of the ~2087 cm^{-1} peak as N-bound thiocyanate is supported by its shift with potential, distortion of the band due to overlap with the S-bound peak and the weakness of the band make a definite assignment difficult. At least one other possible explanation (besides N-bound or solution assignments) exists. The overlap of the weak peak with the S-bound peak may also demonstrate the bipolar nature of the S-bound peak, which increases at more negative potentials. The occurrence of the 2087 cm^{-1} band, which is not seen at

more positive potentials, indicates that there may be a reorientation at more negative potentials.

Additional observations from the silver/thiocyanate system deserve mention. Differences in the spectra versus solution concentration are apparent; peak intensities decrease with decreasing concentration. The biggest change in intensity occurs between the 10mM NaSCN and the 1mM NaSCN spectra. While there are small differences in sample alignment between the experiments, the bulk of the intensity loss is probably due to sub-monolayer coverages at the 1mM NaSCN concentration levels. Although absolute intensities are different with concentration, the trend toward decreasing intensity with decreasing potential is very similar for all three concentrations of NaSCN on silver (see Figure 10). The inability to distinguish an ~2087 cm^{-1} peak at the 1mM NaSCN concentration level may be a function of the low signal/noise observed. No evidence (Figures 2-4) exists for a bridge-bound thiocyanate on the silver surface, which has been reported to appear at a frequency of ~2165 cm^{-1} (18c).

Thus far we have overlooked the possibility that, while we have obtained spectra from the thiocyanate species, infrared surface enhancement has occurred (5). Surface enhancement could help explain the peak broadening observed. In a study of the surface-enhanced Raman (SER) spectrum of thiocyanate on gold, the frequency of the CN stretching band is seen to decrease in intensity and shift to lower frequencies in the range 2100-2130 cm^{-1} with more negative potentials (18). Our data fall in this range and so do other data from thiocyanate on more conventional silver electrodes, where frequencies between 2110 and 2130 cm^{-1} have been reported (17, 28).

Thiocyanate Adsorption on Gold

At a gold surface three apparent peaks are observed from adsorbed

thiocyanate in the 2000-2300 cm^{-1} region (Figures 5-7). In the data from 25mM NaSCN on gold, the peak positions are 2133-2127 cm^{-1}, 2122-2112 cm^{-1}, and 2106-2094 cm^{-1} (wavenumber ranges in response to potentials from +0.2 volts to -0.6 volts). While three peaks are observed in these difference spectra, the appearance of a positive peak at 2112 cm^{-1} at -0.6 volts suggests that there are actually only two absorption bands, nearly superimposed, which are responsible for the observed spectra. The spectra appear to have three peaks since the band which gains intensity at positive potentials is much broader than the band which gains intensity at negative potentials. The fit of these difference spectra to a two-band model show excellent agreement with the data, as described below.

The broader band, gaining intensity at potentials more positive than the zero volt reference, is attributed to S-bound thiocyanate, while the narrower peak with opposite behavior is assigned to N-bound species. The S-bound thiocyanate band may be broader than the band from N-bound thiocyanate because the six polarizable lone pair electrons on the sulfur and the single bond between sulfur and carbon would allow the orientation of the C-S bond with respect to the surface plane to vary. Since the C≡N bond would thereby change its angle and distance to the surface and encounter differences in potential within the double layer region, it would lead to peak broadening. This broadening would not be observed for the N-bound species, since the single, lone-pair orbital on nitrogen would favor a perpendicular orientation with respect to the gold surface.

The postulation of N-bound thiocyanate vibrational frequency in the 2122-2112 cm^{-1} wavenumber range is a higher range than has been previously reported (22, 18a). In the work of Weaver, et al. (18), N-bound thiocyanate has been shown to occur at negative potentials on gold. This was determined both from infrared spectroelectrochemical and SERS results (18). Since SERS results are

known to shift the peak positions to lower frequencies (18), unenhanced spectra may contain peaks due to N-bound species at higher wavenumbers than those seen under SERS conditions. The assignments made from SNIFTIRS data were more difficult due to distortion from the strong solution species band (18a). In these data, the peak postulated to be from N-bound species has a position of 2122-2112 cm^{-1}, but the presence of the N-bound species makes it difficult to make a definite wavenumber assignment for the peak of the S-bound species. Also, shifts in frequency may be distorted by uneven overlap between the two peaks. Finally, these features can be observed in the raw MIRFTIRS spectra where the reference spectrum at 0 volts is not subtracted. However, the changes occurring in both bands are made more apparent in the difference spectra, which clearly show the potential-induced reorientation of the adsorbate.

For 10mM NaSCN (Figure 6), the ranges for the three apparent peaks observed were 2130-2125 cm^{-1}, 2114-2111 cm^{-1}, and 2102-2095 cm^{-1}. From the 1mM NaSCN solution on gold data these ranges were 2129-2123 cm^{-1}, 2117-2108 cm^{-1}, and 2102-2093 cm^{-1}. The signal/noise ratio decreases with decreasing concentration (as in the silver experiments) indicating less coverage with lower concentration of added thiocyanate. While the signal/noise for 1mM NaSCN on gold is better than for 1mM NaSCN on silver, the data are still too noisy to make precise wavenumber assignments. A comparison between the three concentrations of NaSCN on gold shows that $d\nu/dE$ changes very little with decreasing solution thiocyanate concentration for both the N-bound and S-bound thiocyanate. At +0.2 and +0.3 volts, there is a larger, low wavenumber contribution from the peak assigned as the S-bound thiocyanate in the 25mM NaSCN on gold data than in either the 10mM or 1mM NaSCN on gold data. This low wavenumber contribution is either due to the change in peak position of the S-bound peak with concentration, or may support

the contention of Suetaka et al. (5) that a "twinned" thiocyanate group exists at more positive potentials. At more dilute solution concentrations, higher potentials would be required to obtain a sufficient surface concentration of SCN^- ions to form the twinned thiocyanate species.

The existence of a twinned thiocyanate species seems unlikely, however, when two other factors are considered. First, it seems reasonable to expect "twinning" to occur more readily with higher solution concentrations of NaSCN. However, at more negative potentials for all three concentrations, the peak at ~2095 cm^{-1} is the same or larger in negative intensity than the band assigned to S-bound which occurs at ~2125 cm^{-1}. This similarity in intensity implies that the mole ratio of the S-bound species to "twinning" species is the same regardless of concentration, which is unlikely. Second, it is helpful to review the method of data collection. A comparison of the negative potential data in Figures 5-7 shows that, except for signal/noise differences, the trend for the development of negative peaks in what we have labeled the S-bound positions are the same regardless of concentration. In all three experiments, data were collected first from potentials of +0.2 to -0.5 volts. The +0.3 volt data were collected, for the 10mM and 1 mM NaSCN concentrations, after the other data. If, as it appears from the data, the peak possibly arising from twinned species was only weakly formed at +0.2 volts, then the large negative-going peaks seen at more negative potentials are not indicative of the loss of twinned species from the surface. It is not possible to lose surface species which were never there. Because of the method by which the data were collected, we assign the peaks as two overlapping peaks, the narrowest due to N-bound thiocyanate and the broadest due to S-bound thiocyanate.

The results of fitting the 25 mM NaSCN on gold data to a two-band model

using Gaussian band shapes can be seen in Figure 11 and Table II. For reasons cited above, the S-bound absorption band was assumed to be broader than the band due to N-bound thiocyanate. The band widths at half height used for calculations at all potentials were fixed at 15 cm^{-1} for the S-bound and 7 cm^{-1} for the N-bound species. Fitting was optimized by minimizing the sum of the squared residuals. The excellent fit of the two Gaussian band model argues strongly for the presence of two species on the surface. The only region of the data not accommodated by the two-band model is the region around 2020 cm^{-1} in the most negative potential difference spectra; this shoulder can be shown to arise from the frequency shift of the S-bound species absorption relative to the zero-volt reference spectrum (30). The exchange of one surface species for another as a function of surface potential can be readily seen in the relative band intensities plotted in Figure 12. Increased noise in the lower concentration data meant that the data could not be fitted as precisely, so the determination of $d\nu/dE$ would be uncertain. From the fitted data at higher concentrations, for 25 mM NaSCN, $d\nu/dE$ = 16 cm^{-1} V^{-1} for S-bound and $d\nu/dE$ = 10 cm^{-1} V^{-1} for N-bound thiocyanate, which is opposite to the expected trend (where N-bound $d\nu/dE$ > S-bound $d\nu/dE$). While the presence of adsorbed thiocyanate in the background spectrum at zero volts can reduce the magnitude of observed band shifts in difference spectra (30,31), the direction of the band shift <u>is</u> preserved. As shown Figure 13, the S-bound band undergoes large changes in frequency with potential until the potential reaches -0.3 V, below which its vibrational frequency appears to be constant. This latter behavior is actually an artifact of taking a difference spectrum related to the low intensity of the S-bound species in the spectra at large negative potentials (see Figure 12). In this region, the negative-going, S-bound band is dominated by its large contribution

to the zero-volt reference spectrum which is potential-independent.

The clear observation of two species on gold but not on silver has yet to be discussed. Suetaka et al. (4,5) found that the adsorbate spectrum disappeared on gold at more negative potentials than were required to make the spectrum disappear on silver. Apparent differences in the behavior of the two metals may be due to the substantial shift in the potential of zero charge between gold and silver in the $NaClO_4$ electrolyte (29). Considering the different properties of these metals, the variations in the spectra observed due to the metal surface and electronic properties are not surprising. Such properties could be responsible for differences in both the peak positions and intensities for the vibrations of thiocyanate adsorbed on gold and silver.

CONCLUSIONS

The MIRFTIRS technique has been shown to be useful in obtaining information from thiocyanate adsorption on silver and gold within the double-layer region. Its advantages in improved signal-to-noise, surface selectivity, and speed of data collection over other surface spectroelectrochemical techniques demonstrate that the technique should be utilized in future studies of adsorbates. Changes in the ATR substrate used, and the metal films deposited on the surface, will increase the number of applications possible for this method.

The data collected using MIRFTIRS allowed for the recognition and assignment of spectral features from N- and S-bound thiocyanate species on gold surfaces, and for the identification of S-bound species on silver. These assignments differ from earlier assignments, but this can be explained in terms of the better signal/noise from these experiments, and the absence of peaks due to solution species which have obscured earlier spectroelectrochemical results.

ACKNOWLEDGEMENTS

J.M.H. and D.B.P. gratefully acknowledge the Office of Naval Research, the Center for Biopolymers at Interfaces at the University of Utah, and the Alfred P. Sloan Foundation for their support of this work. K.A. acknowledges the Research Corporation and the donors of the Petroleum Research Fund, Administered by the American Chemical Society, for support of this research. The authors also thank Stan Pons and John Daschbach for helpful discussions.

REFERENCES

1) Neugebauer, H.; Neckel, A.; Nauer, G.; Brinda-Konopik, N.; Garnier, F.; Tourillon, G. J. Phys. (Paris) C10, 1983, 12, 44.

2) Neugebauer, H.; Nauer, G.; Brinda-Konopik, N.; Kellner, R. Fresenius Z. Anal. Chem. 1983, 314, 266.

3) Pham, M.-C.; Adami, F.; Lacaze, P.-C; Doucet, J.-P.; Dubois, J.-E. J. Electroanal. Chem. 1986, 201, 413.

4) Hatta, A.; Sasaki; Suetaka, W. J. Electroanal. Chem. 1986, 215, 93.

5) Wadayama, T.; Sakurai, T.; Ichikawa, S.; Suetaka, W. Surf. Sci. 1988, 198, L359.

6) Engstrom, R.C. Anal. Chem. 1984, 56, 890.

7) Kavassalls, C.; Spitler, M. T. J. Phys. Chem. 1983, 87, 3166.

8) Hansen, W. N.; Osteryoung, R. A.; Kuwana, T. J. Am. Chem. Soc. Comm. 1966, 88, 5.

9) Palik, E. D.; Holm, R. T. J. Appl. Phys. 1984, 56 (3), 843.

10) Venkateswara Rao, A., Chazalviel, J.-N.; Ozanam, J. J. Appl. Phys. 1986, 60 (2), 696.

11) Chazalviel, J.-N.; Venkateswara Rao, A. J. Electrochem. Soc. 1987, 134 (5), 1138.

12) Tardella, A.; Chazalviel, J.-N. Phys. Rev. B 1985, 32 (4), 2439.

13) Reed, A. H.; Yeager, E. Electrochim. Acta 1970, 15, 1345.

14) Mark, H. B.; Pons, B. S. Anal. Chem. 1966, 38 (1), 119.

15) Chazalviel, J.-N. Electrochim. Acta 1988, 33 (4), 461.

16) Ashley, K.; Pons. S. Chem. Rev. 1988, 88, 673.

17) Weaver, M.J.; Barz, F.; Gordon, J.G. II; Philpott, M.R. Surf. Sci. 1983, 125, 409.

18) (a) Corrigan, D. S.; Foley, J.K.; Gao, P.; Pons, B. S.; Weaver, M. J. Langmuir 1985, 1, 616. (b) Corrigan, D. S. ; Gao, P.; Leung, L.-W. H.; Weaver, M.J. Langmuir 1986, 2, 744. (c) Corrigan, D.S.; Weaver, M.J. J. Phys. Chem. 1986, 90, 5300.

19) Foley, J. K.; Pons, S.; Smith, J. J. Langmuir 1985, 1, 697.

20) Parry, D.B.; Harris, J.M. Appl. Spectrosc. 1988, 42 (6), 997.

21) Parry, D.B.; Dendramis, A.L. Appl. Spectrosc. 1986, 40 (5), 656.

22) Ashley, K.; Samant, M.G.; Seki, H.; Philpott, M.R., J. Electroanal. Chem., in press.

23) Harrick, N.J. Internal Reflection Spectroscopy Wiley Interscience: New York, 1967.

24) Salzberg, C.D. and Villa, J.J. J. Opt. Soc. Amer. 1957, 47, 244.

25) Downing, H.D. and Williams, D. J. Geophys. Res. 1975, 80 (12), 1656.

26) (a) Hupp, J.T.; Larkin, D.; Weaver, M.J. Surf. Sci. 1983, 125, 429; (b) Larkin, D.; Guyer, K.L.; Hupp, J.T.; Weaver, M.J. J. Electroanal. Chem. 1982, 138, 401.

27) Bockris, J. O'M.; Reddy, A.K.N. Modern Electrochemistry, Vol. 2; Plenum Press: New York, 1973, Chapter 3.

28) Wetzel, H.; Gerischer, H.; Pettinger, B. Chem. Phys. Lett. 1981, 80, 159.

29) (a) Argade, S.A.; Gileadi, E. in Electrosorption; Gileadi, E., Ed. Plenum Press: New York, 1967. (b) Perkins, R.S.; Andersen, T.N. in Modern Aspects of Electrochemistry, Vol. 5; Bockris, J.O'M.; Conway, B.E., Eds. Plenum Press: New York, 1969.

30) Brown, C.W.; Lynch, P.A.; Obremski, R.J. Appl. Spectrosc. 1982, 36, 539.

31) Rao, B.; Stobie, R.W.; Dignam, M.J. J. Chem. Soc. Faraday Trans. II, 1975, 71, 654.

FIGURE LEGENDS

1) Detail of the electrochemical ATR FTIR cell. A shows the O-ring position in the cell, B is the silicon prism, C is a teflon flow cell chamber which is not filled in this experiment, D indicates the aluminum supports, and E is the electrochemical flow cell chamber. A more complete view of E in seen in the top view. Here, F is the reference electrode (SCE) which fits through a hole in the back of E (as seen in the exploded view). G is the platinum secondary electrode, H indicates the metal-coated side of the infrared substrate, I is a teflon protrusion used to hold G in place, and J is the liquid chamber itself.

2) Difference spectra of 25mM NaSCN in aqueous 0.15M NaClO4 on silver. The background reflectance spectrum used for ratioing is the filled, nitrogen purged cell at a potential of 0 volts. The potentials vs. SCE are as follows A) +0.2 V, B) +0.1 V, C) -0.1 V, D) -0.2 V, E) -0.3 V, F) -0.4 V, G) -0.5 V, H) -0.6 V.

3) Same as Figure 2 with a NaSCN concentration of 10mM.

4) Same as Figure 2 with a NaSCN concentration of 1mM.

5) Difference spectra of 25mM NaSCN in aqueous 0.15M $NaClO_4$ on gold. The background spectrum subtracted is the filled, nitrogen purged cell at a potential of 0 volts. The potentials vs. SCE shown are as follows A) +0.2 V, B) +0.1 V, C) -0.1 V, D) -0.2 V, E) -0.3 V, F) -0.4 V, G) -0.5 V.

6) Same as Figure 5 with a NaSCN concentration of 10mM. The potentials vs. SCE shown are A) +0.3 V, B) +0.2 V, C) +0.1 V, D) -0.1 V, E) -0.2 V, F) -0.3 V, G) -0.4 V, H) -0.5 V.

7) Same as Figure 5 with a NaSCN concentrations of 1mM. The potentials vs. SCE shown are the same as in Figure 6 with the addition of I) -0.6 V.

8) Expanded difference spectra of the 25mM NaSCN system in aqueous 0.15M $NaClO_4$ at a potential of -0.5 V (vs. SCE) on A) gold and B) silver.

9) Difference spectra of 25mM NaSCN in aqueous 0.15M $NaClO_4$ on silver at higher positive potentials. The potentials vs. SCE shown are A) +0.4 V and B) +0.3 Volts.

10) Changes in intensity with potential (vs. SCE) for three concentrations of NaSCN at silver; A) 25 mM NaSCN, B) 10 mM NaSCN, C) 1 mM NaSCN.

11) Difference spectra from 25 mM NaSCN solution on gold (points) fitted to a Gaussian peak shape (line). Data are from various potential vs. SCE: A) +0.2 V, B) -0.1 V, C) -0.2 V, D) -0.3 V, E) -0.4 V, F) -0.5 V.

12) Plot of intensity vs. potential for fitted data from 25 mM NaSCN on gold experiment. + = N-bound, |=| = S-bound.

13) Plot of peak position vs. potential for fitted data from 25 mM NaSCN on gold experiment. + = N-bound, |=| = S-bound.

Table I. Frequency and intensity potential dependence of S-bound C-N stretch due to thiocyanate species adsorbed on silver. Concentrations shown are 25 mM NaSCN, 10 mM NaSCN, and 1 mM NaSCN. Data not shown were too weak to include.

	25mM		10mM		1mM	
Potential	cm^{-1}	intensity	cm^{-1}	intensity	cm^{-1}	intensity
+0.2 V	2124	0.0050	2124	0.0045	2121	0.00060
+0.1 V	2123	0.0025	2122	0.0033		
-0.1 V	2117	-0.0022				
-0.2 V	2116	-0.0039	2116	-0.0022	2118	-0.00028
-0.3 V	2116	-0.0045	2116	-0.0029	2117	-0.00034
-0.4 V	2115	-0.0049	2114	-0.0034	2118	-0.00043
-0.5 V	2115	-0.0049	2114	-0.0033	2117	-0.00044
-0.6 V	2114	-0.0048	2114	-0.0033	2118	-0.00047

Table II. Frequency and intensity potential dependence of S- and N-bound C-N thiocyanate stretch from gaussian fit of 25 mM NaSCN on gold data. Data in parentheses fit an order of magnitude worse than other data.

	25mM S-bound		25mM N-bound	
Potential	cm^{-1}	intensity	cm^{-1}	intensity
+0.2 V	2119.7	0.0047	2119.2	-0.0042
+0.1 V	(2116.0	0.0029	2118.5	-0.0029)
-0.1 V	2118.0	-0.0033	2114.6	0.0030
-0.2 V	2115.3	-0.0054	2113.9	0.0052
-0.3 V	2109.8	-0.0082	2112.8	0.0087
-0.4 V	2109.8	-0.0092	2112.3	0.0120
-0.5 V	2110.0	-0.0093	2111.0	0.0125

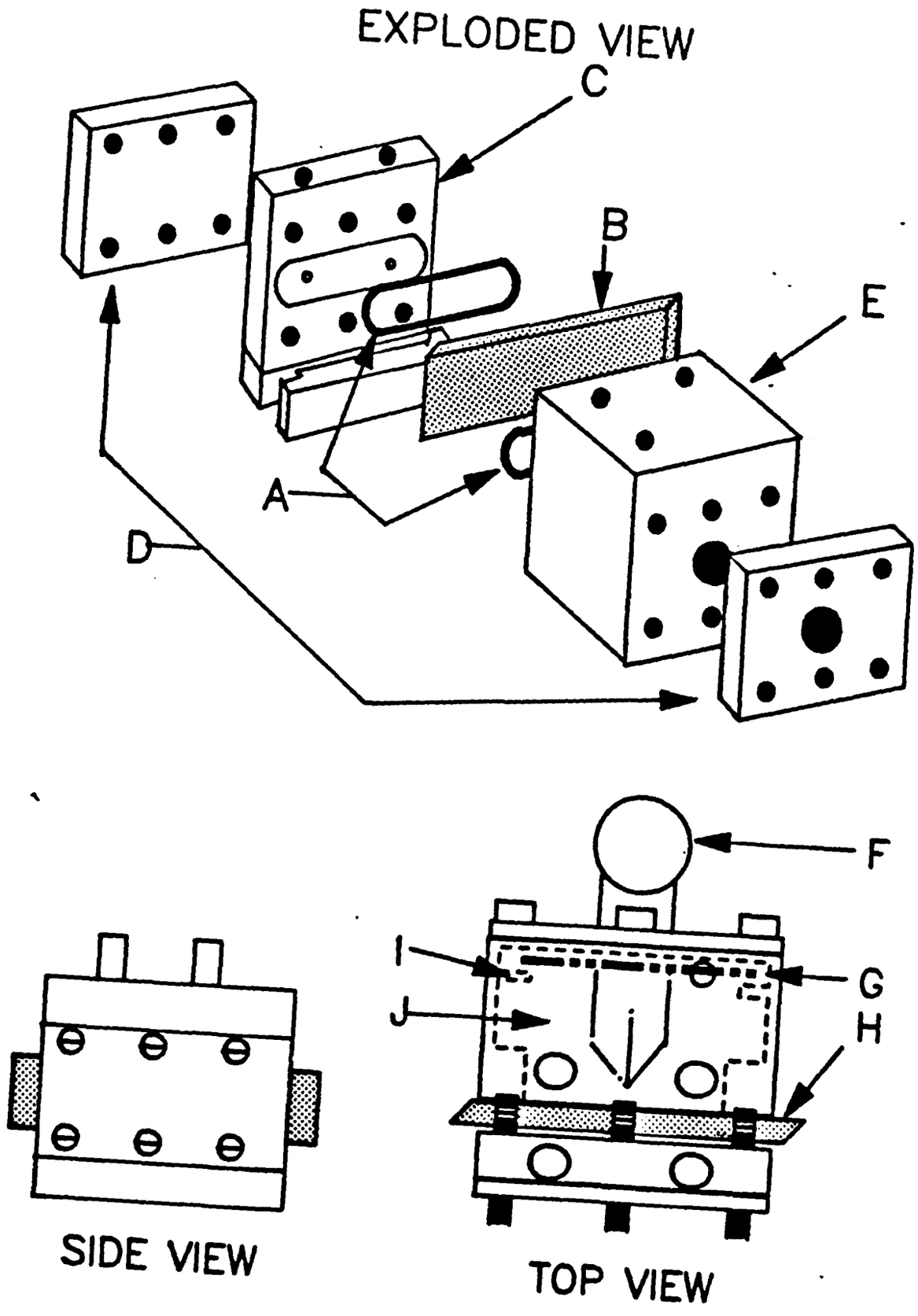

Fig. 1

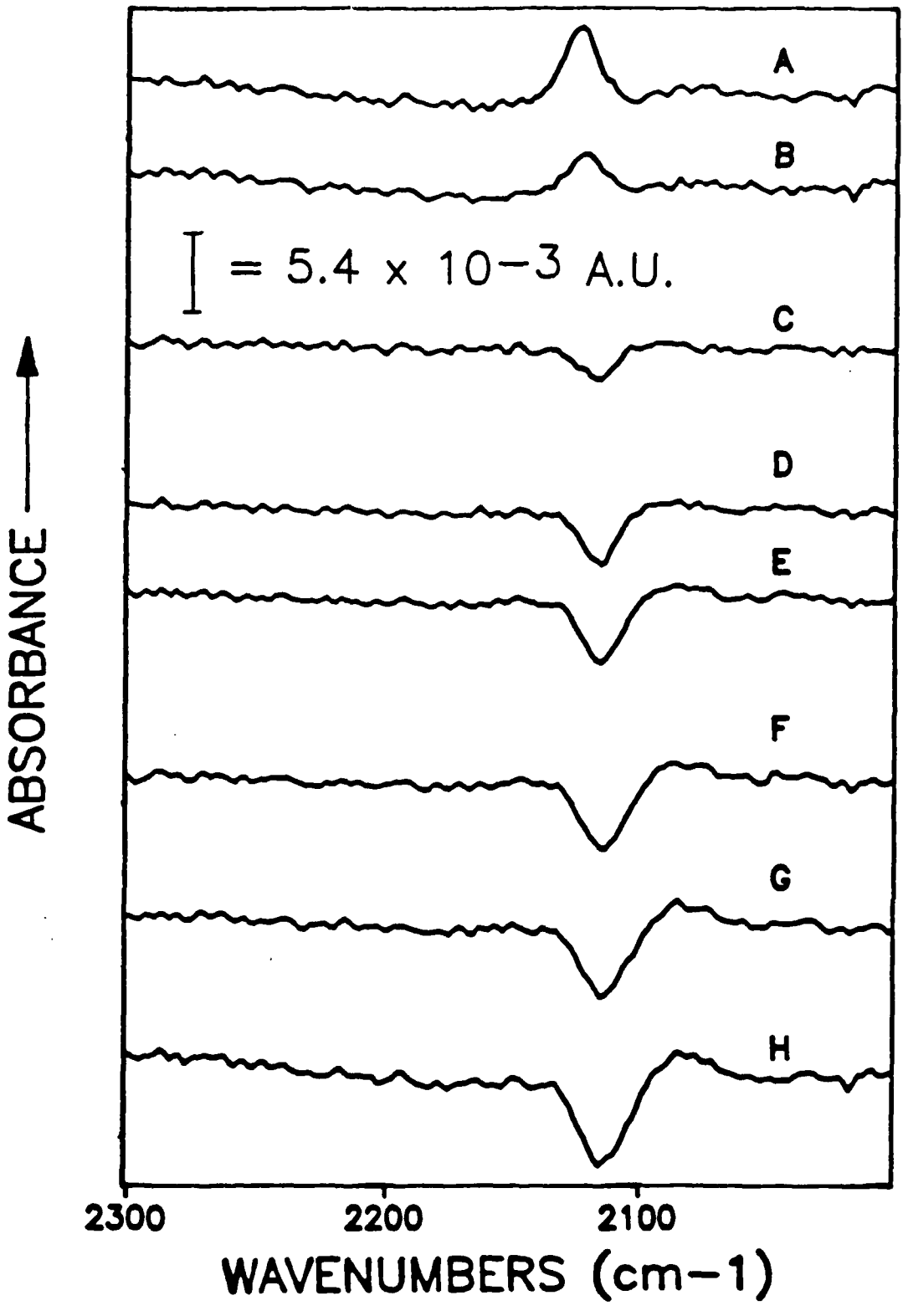
A
B
I = 5.4 x 10−3 A.U.
C
D
E
F
G
H
ABSORBANCE
2300
2200
2100
WAVENUMBERS (cm−1)

Fig 2.

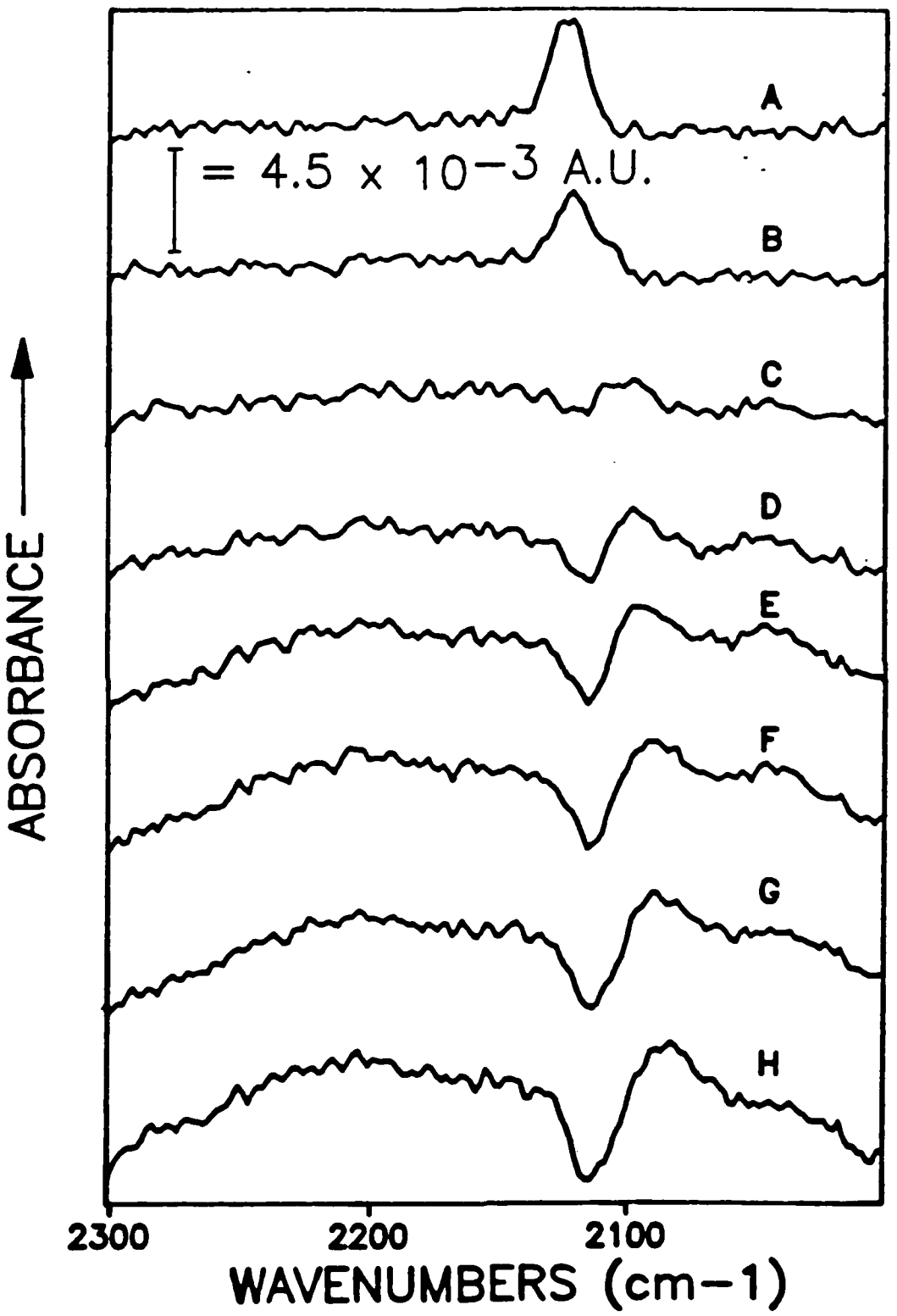
A
= 4.5 x 10−3 A.U.
B
C
D
E
F
G
H
ABSORBANCE
2300
2200
2100
WAVENUMBERS (cm−1)

Fig 3.

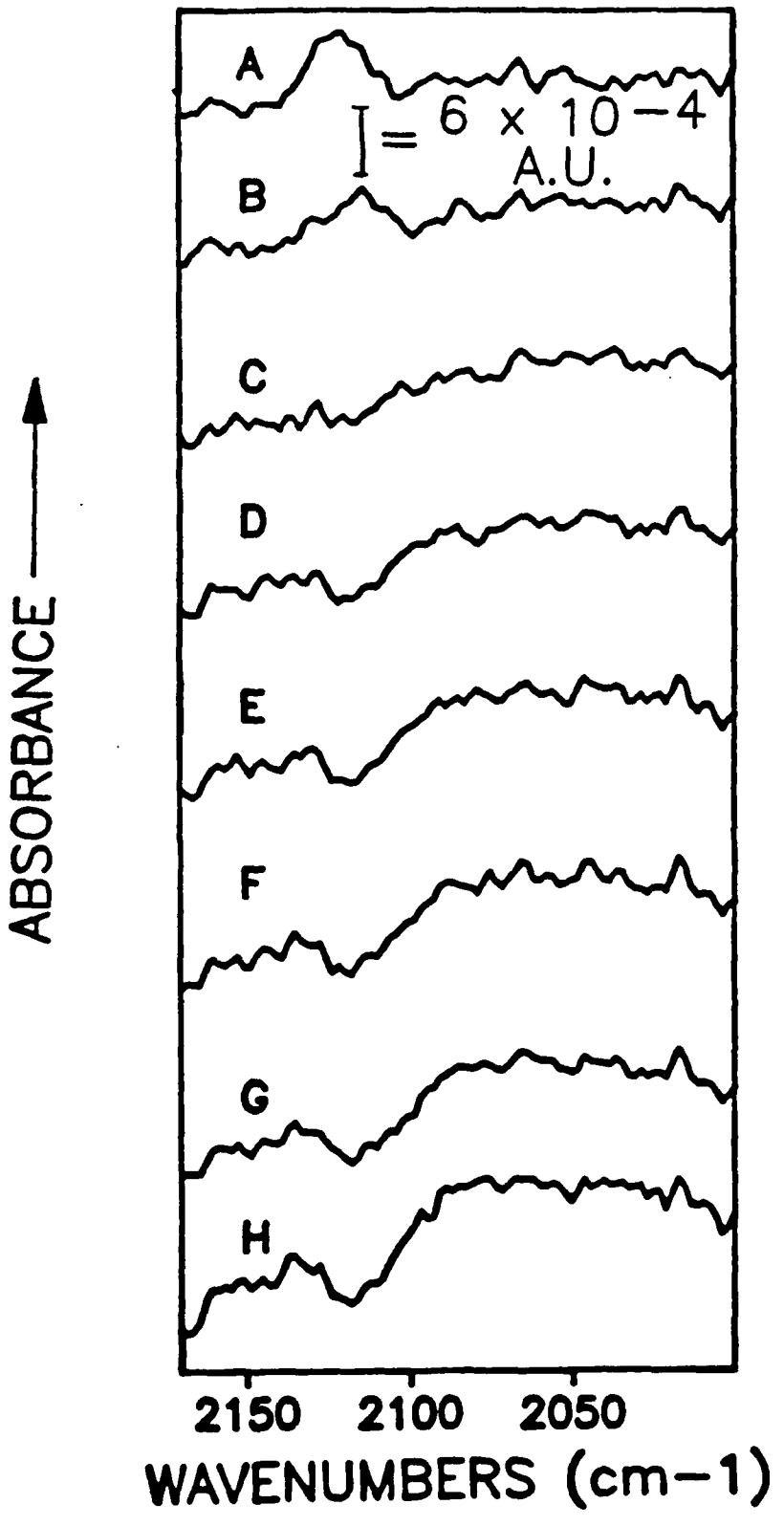
A
B
C
D
E
F
G
H
I = 6 x 10−4 A.U.
ABSORBANCE
2150
2100
2050
WAVENUMBERS (cm−1)

Fig. 4

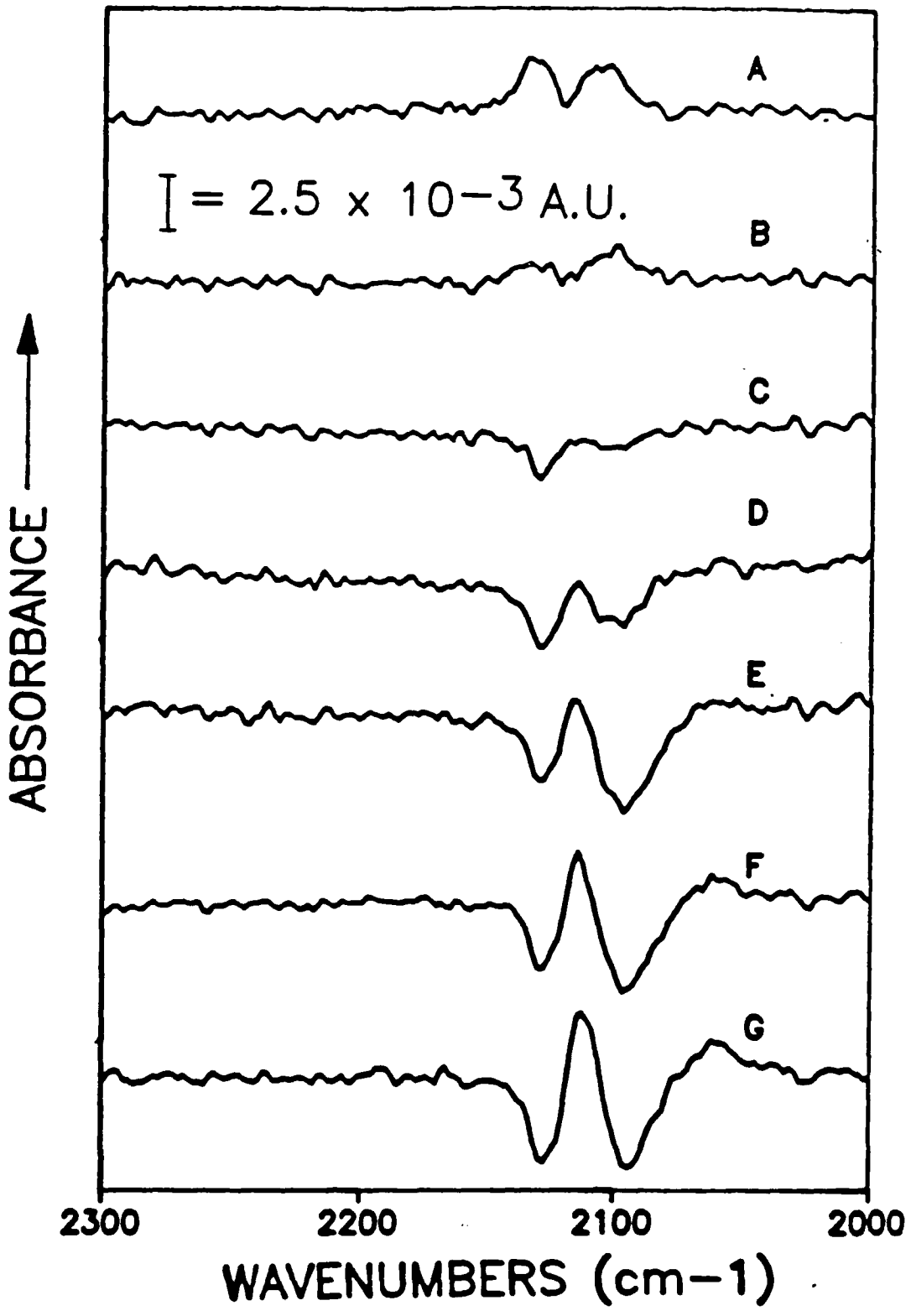
A
I = 2.5 x 10−3 A.U.
B
C
D
E
F
G
ABSORBANCE
2300
2200
2100
2000
WAVENUMBERS (cm−1)

Fig. 5

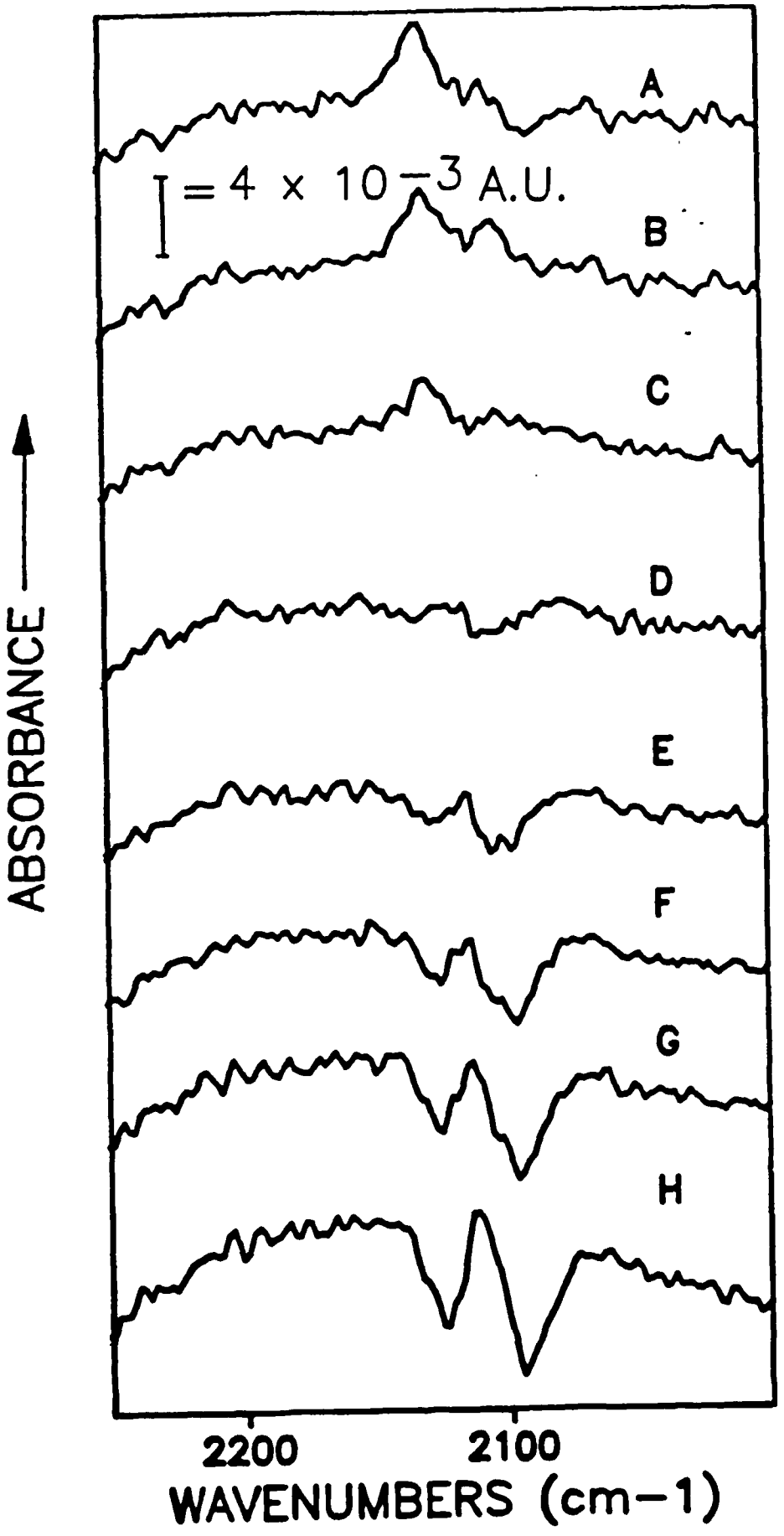

Fig 6

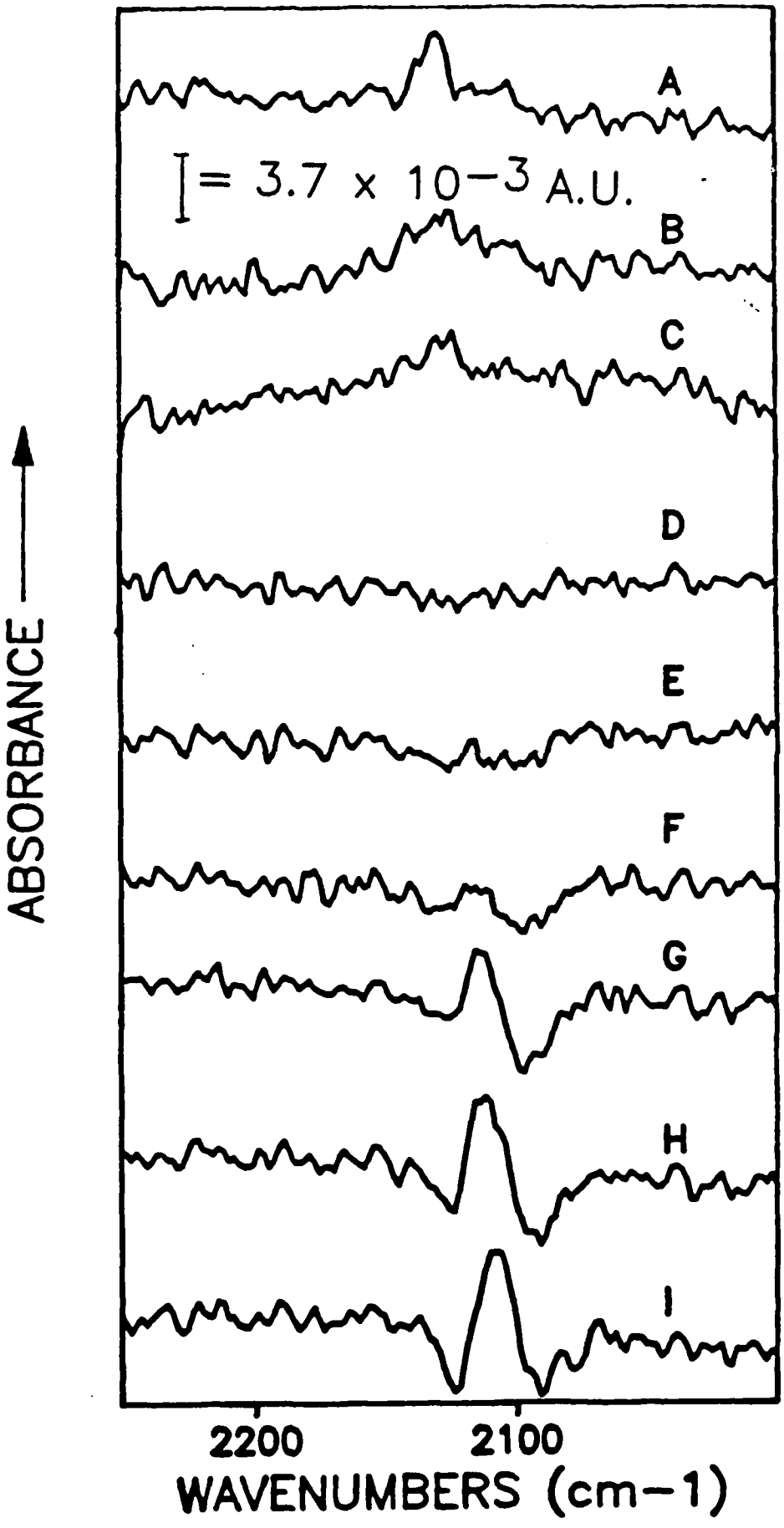
A
I = 3.7 x 10−3 A.U.
B
C
D
E
F
G
H
I
ABSORBANCE
2200
2100
WAVENUMBERS (cm−1)

Fig. 7

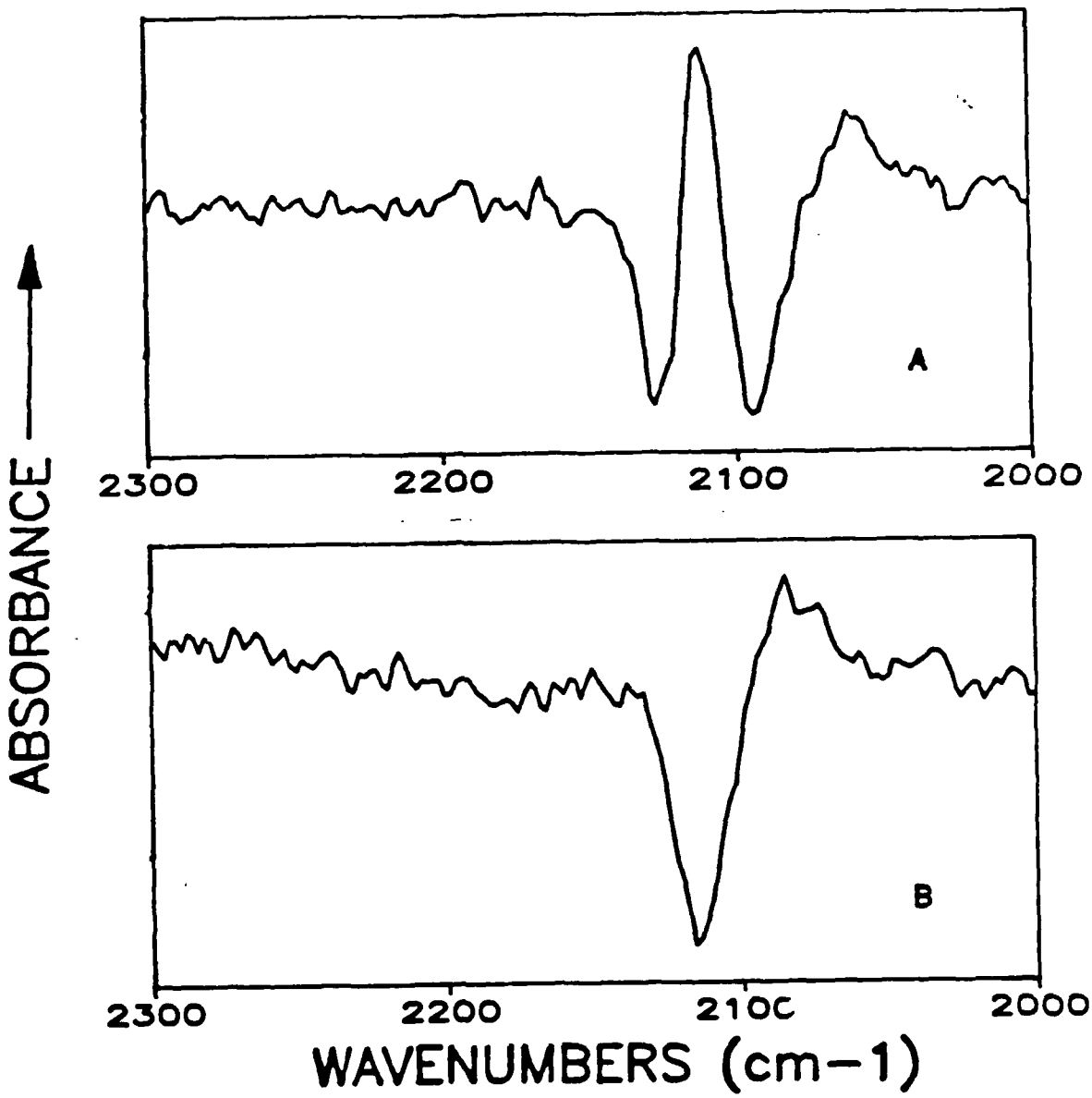
ABSORBANCE
A
2300
2200
2100
2000
B
2300
2200
210C
2000
WAVENUMBERS (cm−1)

Fig. 8

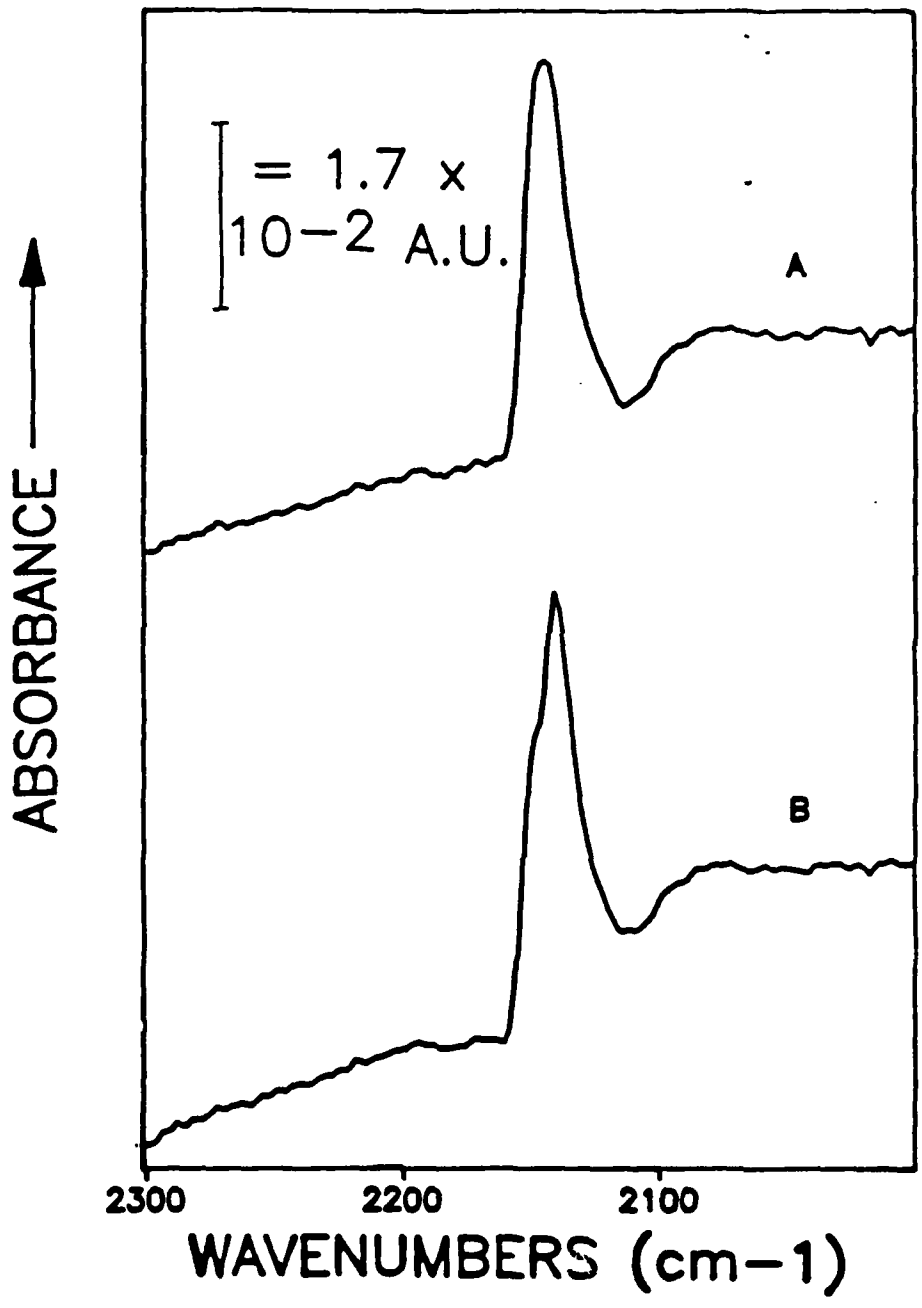

Fig. 9

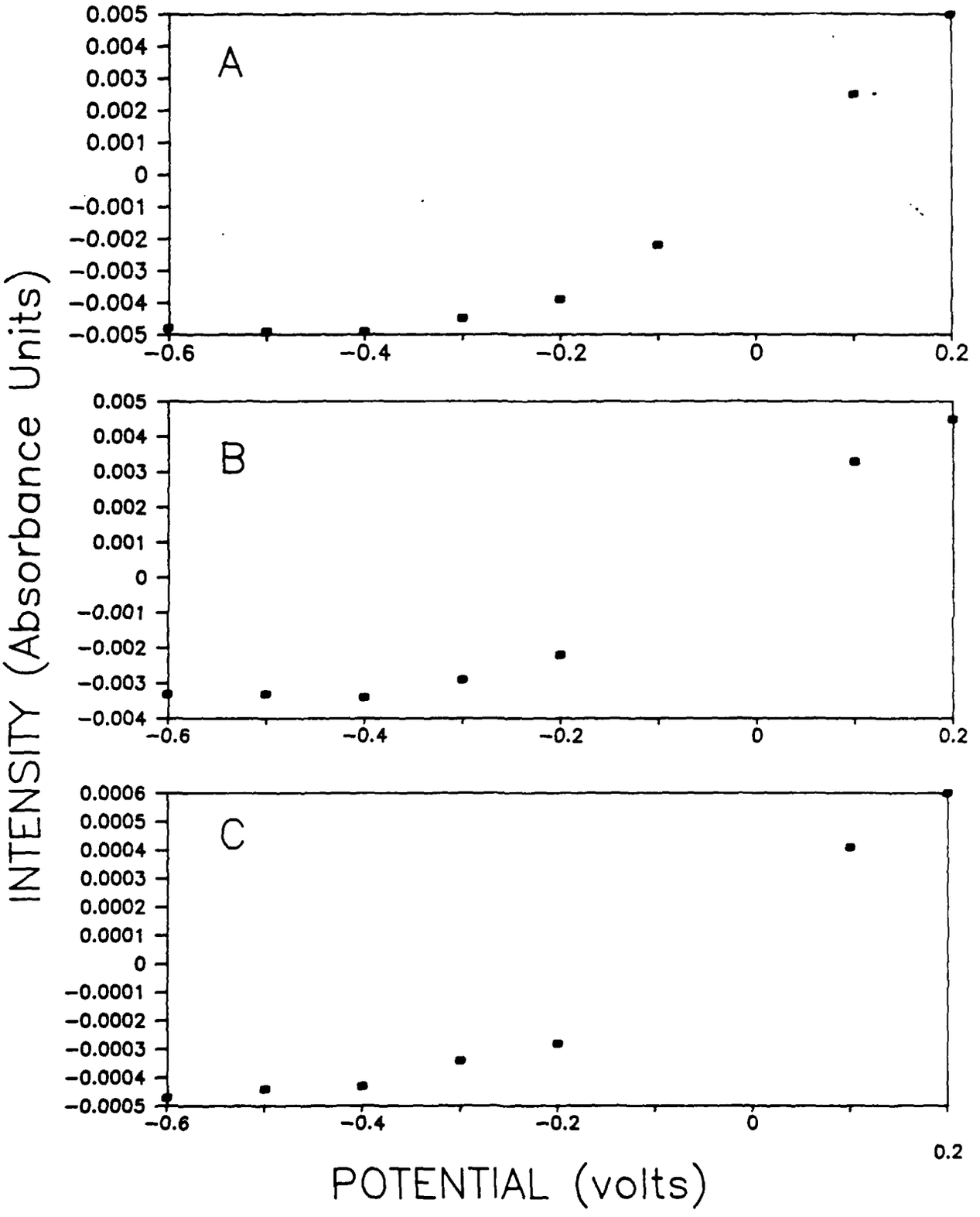
A
B
C
INTENSITY (Absorbance Units)
POTENTIAL (volts)
0.005
0.004
0.003
0.002
0.001
0
-0.001
-0.002
-0.003
-0.004
-0.005
-0.6
-0.4
-0.2
0
0.2
0.0006
0.0005
0.0004
0.0003
0.0002
0.0001
-0.0001
-0.0002
-0.0003
-0.0004
-0.0005

Fig. 10

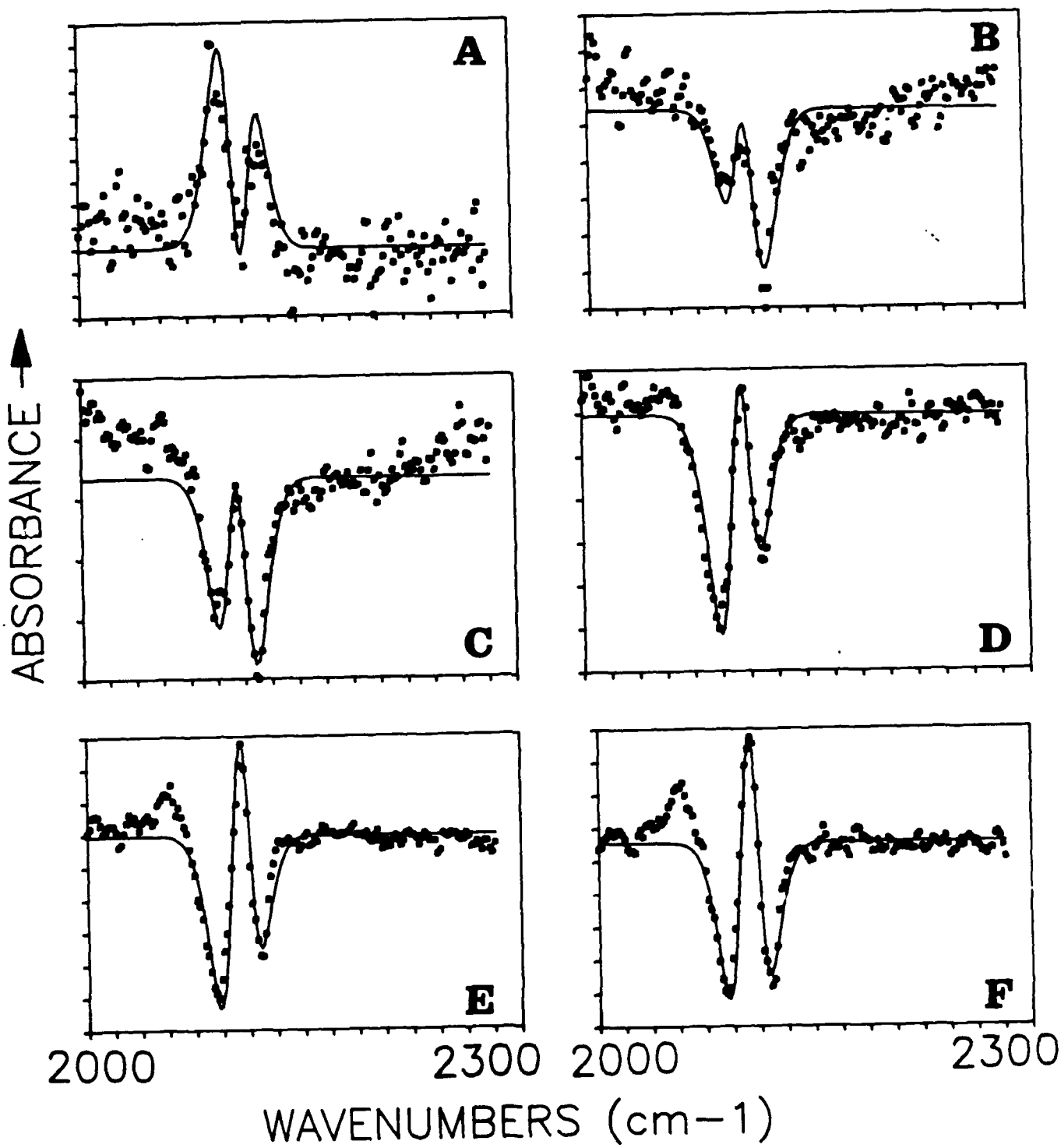

Fig. 11

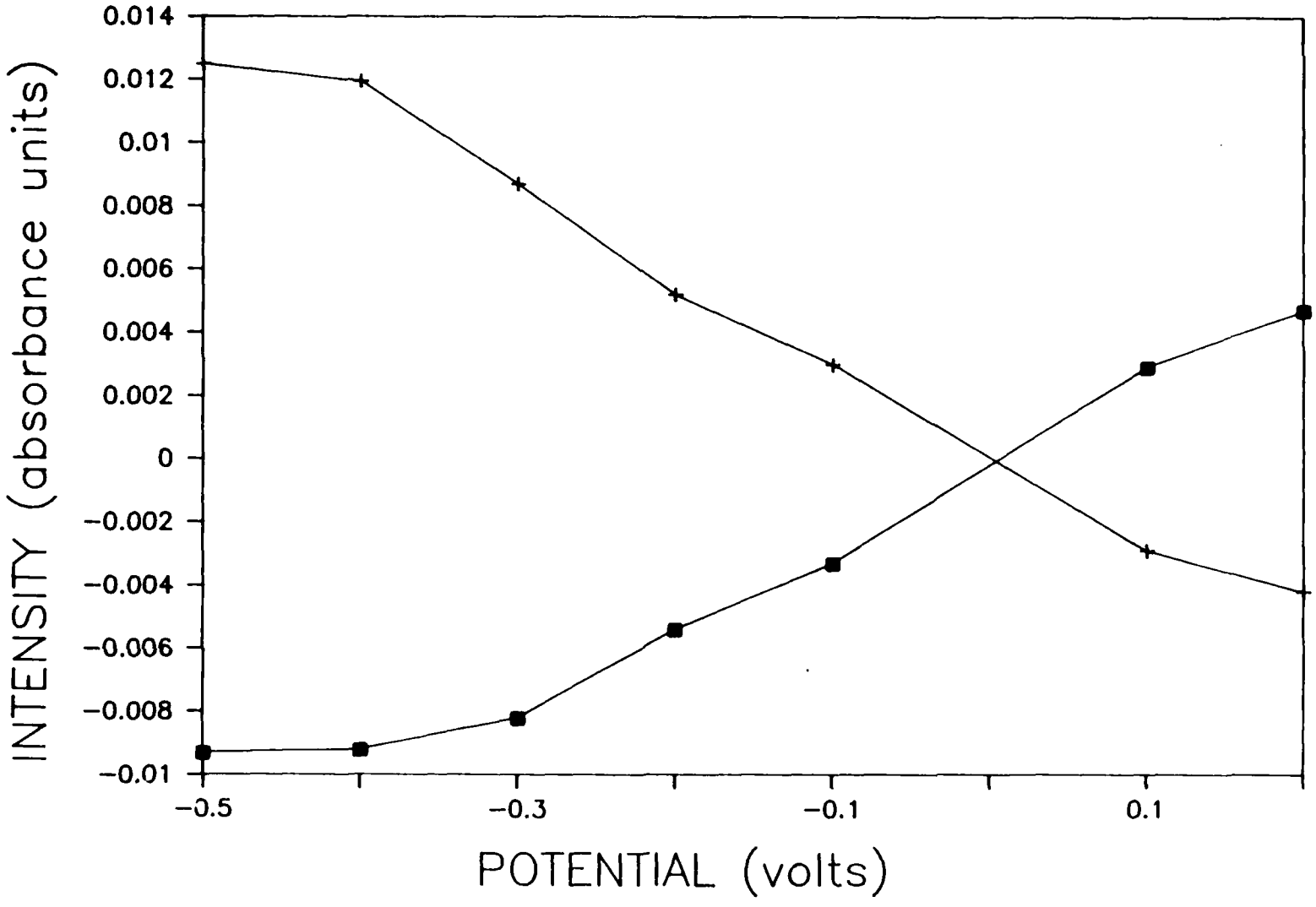
INTENSITY (absorbance units)
0.014
0.012
0.01
0.008
0.006
0.004
0.002
0
−0.002
−0.004
−0.006
−0.008
−0.01
−0.5
−0.3
−0.1
0.1
POTENTIAL (volts)

Fig 8

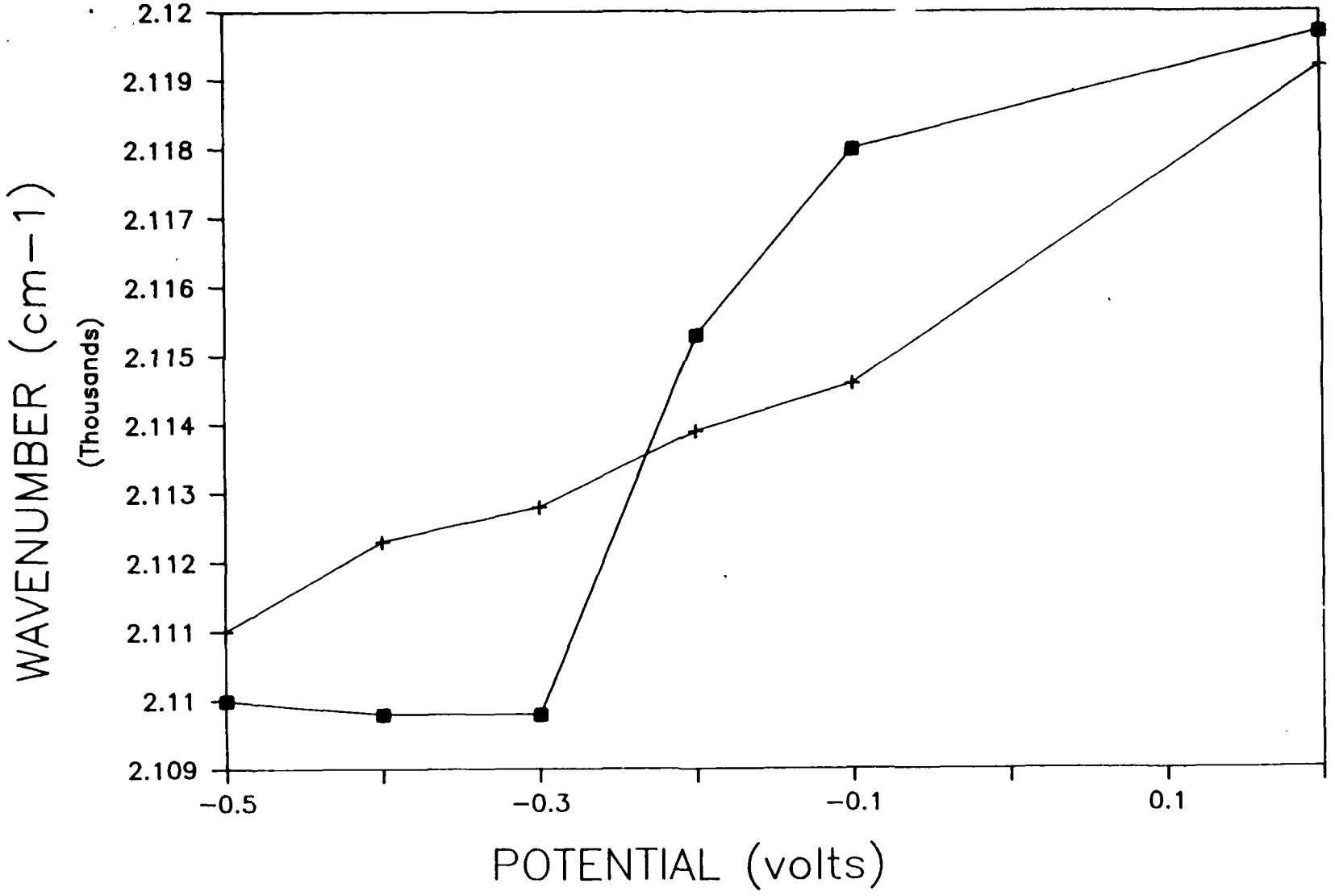
WAVENUMBER (cm−1)
(Thousands)
2.12
2.119
2.118
2.117
2.116
2.115
2.114
2.113
2.112
2.111
2.11
2.109
−0.5
−0.3
−0.1
0.1
POTENTIAL (volts)